Supporting Information

Pruning the ALS-associated protein SOD1 for in-cell NMR.

Jens Danielsson, Kohsuke Inomata, Shuhei Murayama, Hidehito Tochio, Lisa Lang, Masahiro Shirakawa and Mikael Oliveberg*

[1]Department of Biochemistry and Biophysics, Arrhenius Laboratories of Natural Sciences, Stockholm University, S-106 91 Stockholm, Sweden. [2]Department of Molecular Engineering, Graduate School of Engineering, Kyoto University, Katsura, Kyoto 615-8510, Japan. [3]Laboratory for Cell Dynamics Observation, Quantitative Biology Center, RIKEN, OLABB, Osaka University 6-2-3, Furuedai, Suita, Osaka 565-0874, Japan

A. Supporting Figures S1-S8.

B. Supporting Material and Methods.

A. Supporting Figures

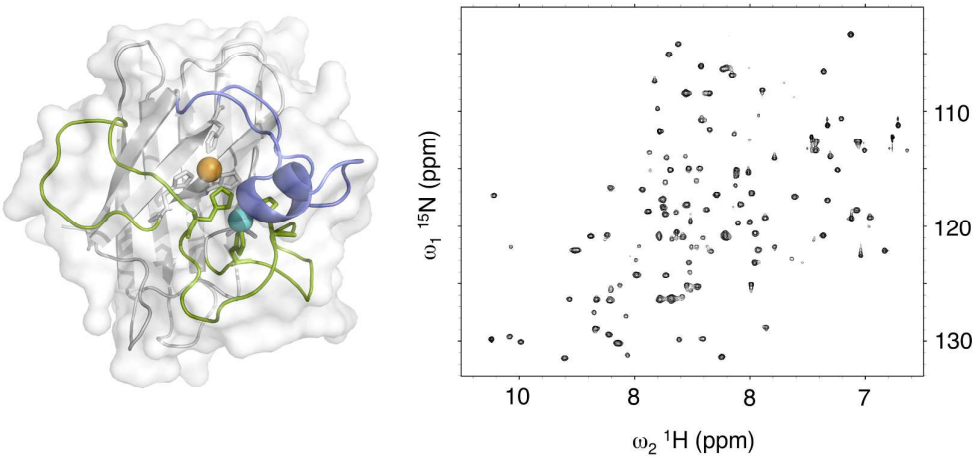

Figure S1. A. The monomeric, enzymatically active variant of superoxide dismutase 1 (holoSOD1^{pwt}) has an immunoglobulin-like scaffold harbouring two long functional loops, loop IV (green) and loop VII (blue). Loop IV is directly involved in coordinating the structurally important zinc ion (blue sphere) as well as the enzymatically redox-active copper ion (orange sphere). Loop VII is highly charged and is involved in substrate direction. Together, loops IV and VII build up a stable scaffold around the active-site copper. B. The ^{1}H-^{15}N-HSQC NMR spectrum of holoSOD1^{pwt} shows a highly dispersed, narrow line-width pattern in agreement with a fully folded, fast tumbling and rigid protein.

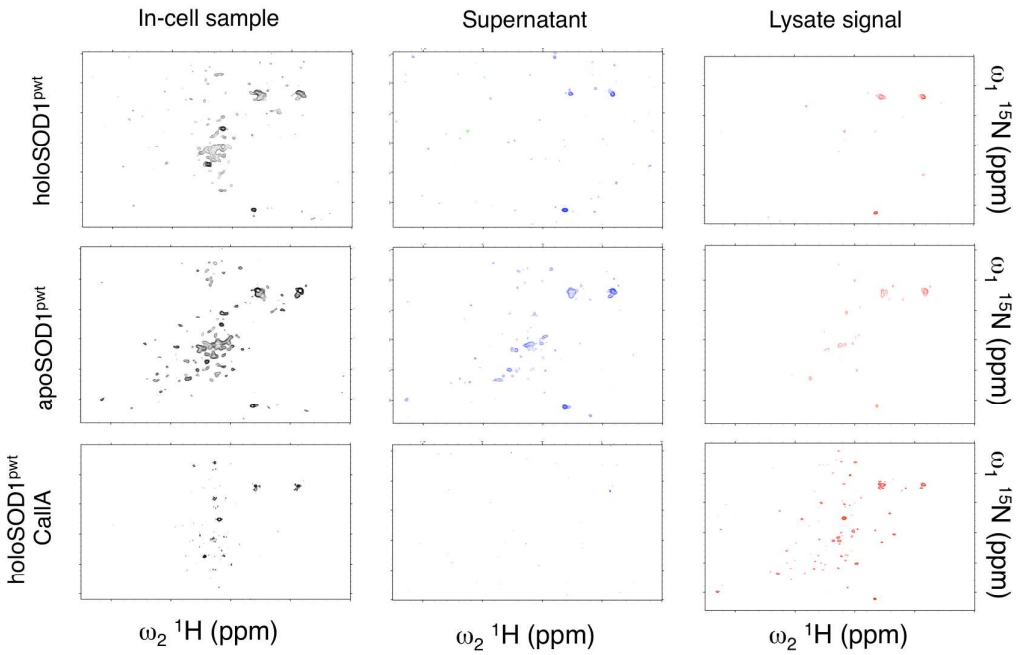

Figure S2. In-cell NMR data and extra-cellular controls, using the CCP R8 attached to C39 on the SOD1 surface. ^{1}H-^{15}N HMQC NMR spectra of HeLa cells treated with holoSOD1^{pwt} show only weak and broad signals, assigned to the cellular background (top left). No detectable signal was found in the supernatant (top center) or in the lysate (top right) showing that no, or only small amount, of holoSOD1^{pwt} is delivered into the cells. Removal of the metals to obtain apoSOD1^{pwt} reduces both protein stability and rigidity but fails also to yield useful in-cell NMR signal (middle row). Finally, in order to rule out the involvement of promiscuous CPP conjugation and non-native disulphide linkage, the completely cysteine depleted construct holoSOD1^{CallA} was tested. This variant is also a good mimic for the reduced holoSOD1^{pwt} protein. A weak signal was achieved (bottom left) that increased in the lysate spectrum (bottom right), indicating that the signal stems from the cellular interior. However, the signal is still too weak for analysis.

SOD1^{pwt}-R8, net charge: **+ 0.6** C-RRRRRRRR

ATKAVAVLKGDGPVQGIINFEQKESNGPVKVWGSIKGLCEGLHGFHVHEEEDNTAG
CTSAGPHFNPLSRKHGGPKDEERHVGDLGNVTADKDGVADVSIEDSVISLSGDHAII
GRTLVVHEKADDLGKGGNEESTKTGNAGSRLACGVIGIAQ

SOD1^{pwt} CallA-R8, net charge: **+ 0.7** C-RRRRRRRR

ATKAVAVLKGDGPVQGIINFEQKESNGPVKVWGSIKGLCEGLHGFHVHEEEDNTAG
ATSAGPHFNPLSRKHGGPKDEERHVGDLGNVTADKDGVADVSIEDSVISLSGDHAII
GRTLVVHEKADDLGKGGNEESTKTGNAGSRLAAGVIGIAQ

SOD1$^{\Delta IV\Delta VII}$-R8, net charge: **+ 5.4** C-RRRRRRRR

ATKAVAVLKGDGPVQGIINFEQKESNGPVKVWGSIKGLCEGLHGFHVHGAGGDL
GNVTADKDGVADVSIEDSVISLSGDHSIIGRTLVVHEKAGAGAGSRLASGVIGIAQ

SOD1$^{\Delta IV\Delta VII}$-TAT, net charge: **+ 5.4** C- YGRKKRRQRRR

ATKAVAVLKGDGPVQGIINFEQKESNGPVKVWGSIKGLCEGLHGFHVHGAGGDL
GNVTADKDGVADVSIEDSVISLSGDHSIIGRTLVVHEKAGAGAGSRLASGVIGIAQ

Figure S3. The sequences, CPP-conjugation site, and overall charge of the constructs analysed in this study.

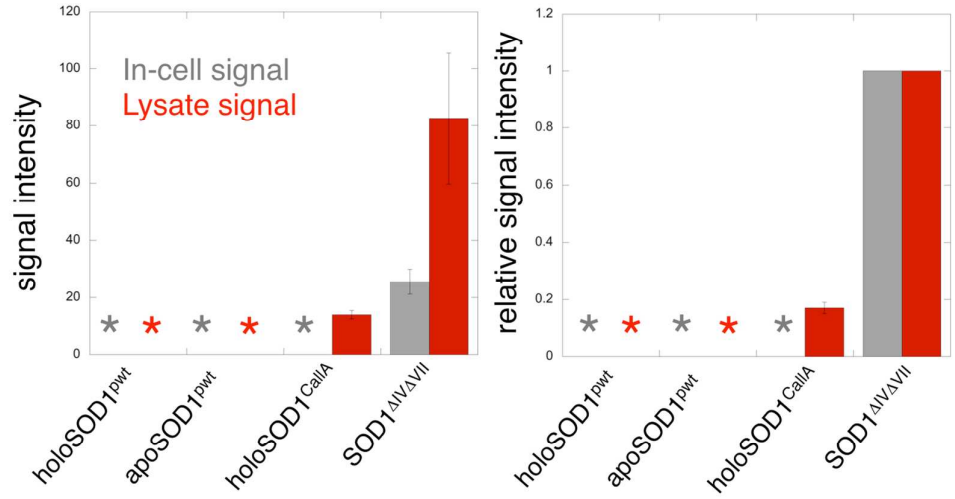

Figure S4. Left. Signal intensities from in-cell NMR experiments of the various SOD1 constructs analysed in this study. In each spectrum the intensity of twelve non-overlapping and well-resolved cross-peaks were determined. Constructs or conditions yielding too low signal are marked with an asterisk. If no signal was detected in the lysate sample we assumed that there was no in-cell protein delivery. Right. Signal intensities normalised to the values of the SOD1$^{\Delta IV\Delta VII}$ construct. The relatively low lysate signal from the holoSOD1^{CallA} construct indicates that low transduction yield.

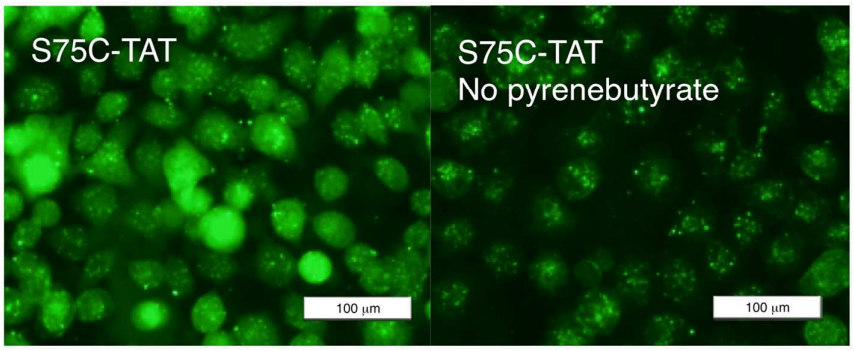

Figure S5. Fluorescence micrographs showing the cellular localization of TAT-delivered apoSOD1$^{\Delta IV\Delta VII}$. Left. Transduction yield is independent of TAT anchoring position, where both C39 (c.f. article Figure 2) and C75 yield predominantly cytosolic apoSOD1$^{\Delta IV\Delta VII}$ localization in the presence of pyrenebuturate. Right. Omitting pyrenebuturate in the transduction protocol leaves mainly granular distribution of apoSOD1$^{\Delta IV\Delta VII}$. These cells fail also to produce in-cell NMR signal.

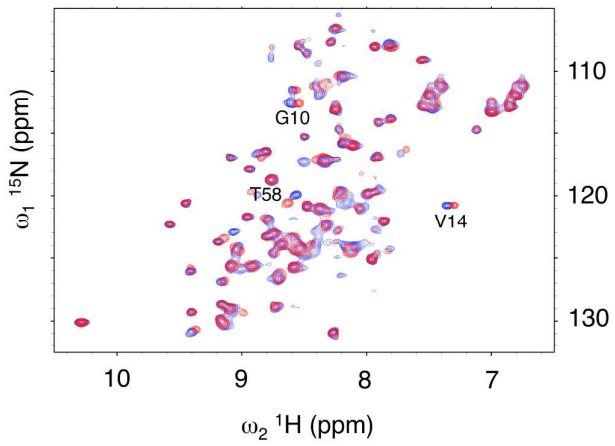

Figure S6. The chemical-shift changes induced by conjugation of the TAT-peptide to apoSOD1$^{\Delta IV\Delta VII}$. The spectra indicate small but significant perturbations on the protein surface but no overall structural effects (c.f. article Figure 1). The most perturbed cross-peaks were used to indicate that the CPP is reductively cleaved off the protein upon transfer into the cells.

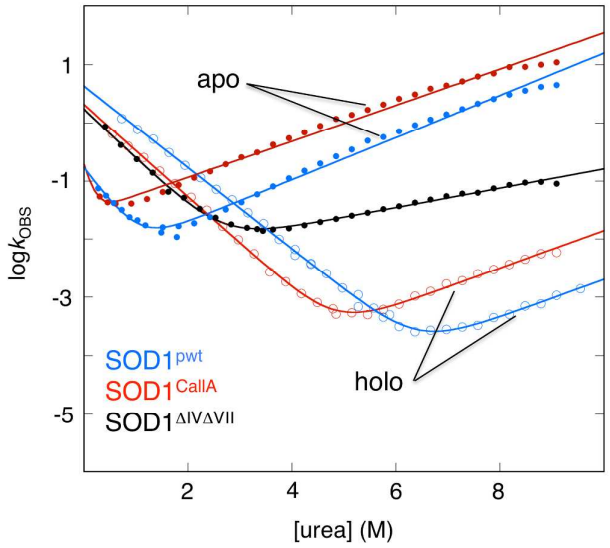

Figure S7. Chevron plots of holoSOD1^{pwt}, apoSOD1^{pwt}, apoSOD1^{CallaA}, holoSOD1^{CallaA} and apoSOD1$^{\Delta IV\Delta VII}$ showing fits of logk_f and logk_u from Equation S1. Neither the protein stability nor the folding kinetics affects the CPP-mediated transduction of SOD1.

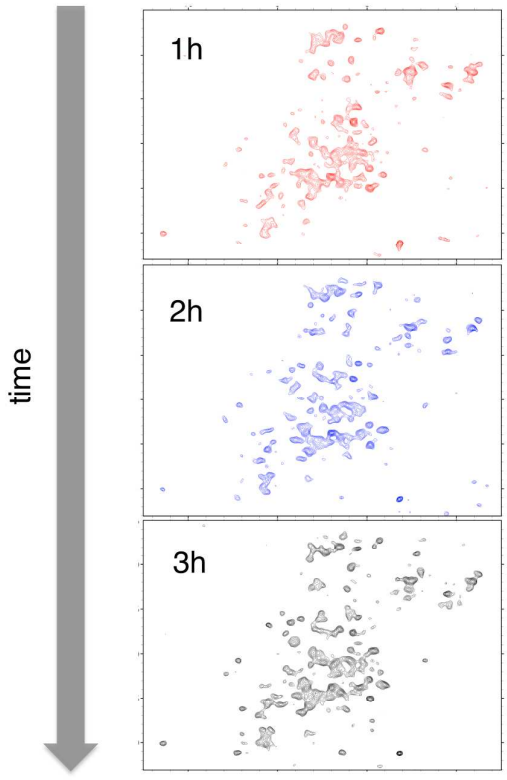

Figure S8. Time course of the in-cell NMR spectrum of apoSOD1$^{\Delta IV\Delta VII}$. The sample was inserted into the NMR spectrometer and three consecutive spectra were recorded, one hour each. Although small changes can be seen, the characteristic signature of the folded protein sustains over three hours. The observed changes in chemical shifts and signal intensities show no consistent drift in pH during the total 3 h acquisition time in the NMR tube, i.e. the changes do not comply with the pattern observed during pH titration (c.f. article Figure 4).

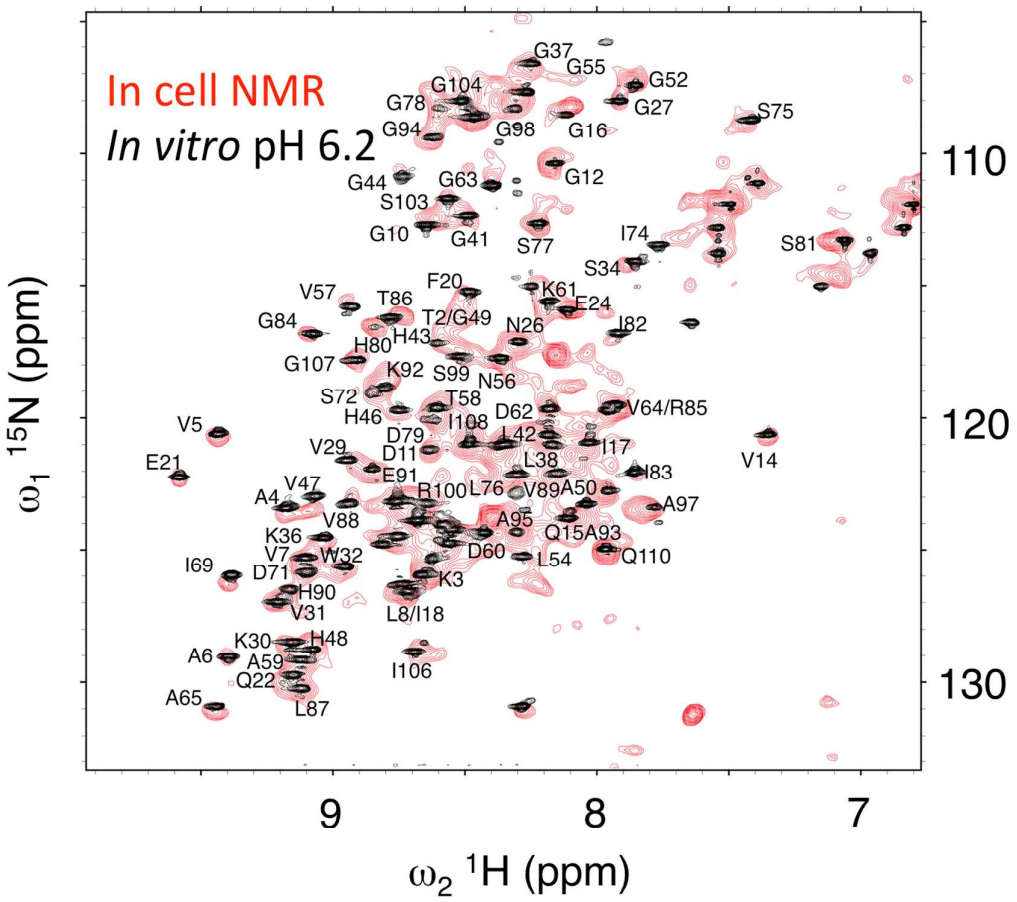

Figure S9. Overlay of the in-cell SOFAST-HMQC spectrum of apoSOD1$^{\Delta IV\Delta VII}$ and the corresponding HMQC spectrum recorded *in vitro* at 37 °C K and pH 6.2. The spectral match indicates that chemical-shift differences induced by cell internalization arise from in-cell acidification.

B. Supporting Materials and methods

Protein preparation. Mutagenesis, expression and purification were performed as in [1,2]. The cysteine moieties of the cell-penetrating peptides (R8: C-RRRRRRRR and TAT: C- YGRKKRRQRRR) were activated by DTDP (2,2'-dithiodipyridine), by mixing 10 mg peptide (dissolved in 200 µl of 2 M acetic acid and 4.6 mg DTDP) with 100 µl isopropanol and subsequent incubation overnight on shaker at room temperature. The activated peptide was purified by RP-HPLC and lyophilized twice. The ^{15}N-labelled protein was conjugated to the activated peptide as described in Inomata *et al.*[3] by mixing 0.2 molar equivalents of peptide with 1 molar equivalent protein on ice. The mixture was then incubated on ice for 5 minutes and the procedure repeated five times for full conjugation. Each step was checked by non-reducing gel. The conjugated protein was separated from the peptide by gel chromatography and concentrated to 1 mM by centrifugation in concentration cell.

In-cell NMR sample preparation. HeLa cells were plated onto 90 mm circular plates and grown until 95 % confluent cell layer was achieved in incubator at 5 % CO_2. Transduction of CPP conjugated proteins into HeLa cells was according to the protocol in Inomata *et al.* [3]. In short, the cells were washed twice and treated by 250 µM pyrenebutyrate (PB) during 5 min incubation under 5 % CO_2 at 37 °C. After incubation, the cells were washed and incubated for 40 min under 5% CO_2 at 37 °C for recovery. The protein transduction was performed in four cycles of cell exposure, in 0.3 mM PB and 0.25 mM CPP-conjugated protein for 10 minutes, each followed by 40 min cell recovery. The cells were then harvested by addition of Trypsin/EDTA to

release the cells from the plate. The cells were finally washed and centrifuged gently at 200 g for 5 minutes twice, before transferred to a 4 mm NMR shigemi tube.

NMR spectroscopy. NMR assignment was as described in Danielsson *et al.* [2] and by using a series of HSQC spectra at various pH values ranging from 6.2 to 8.0. In this way the majority of resonances were assigned. The few cross-peaks that could not be unambiguously assigned due to overlap were left out in the analysis. Samples were transferred into a 700 MHz spectrometer with a cryo-probe in a 4 mm shigemi NMR tube without inserted plunger. A series of three SOFAST-HMQC [4] with 32 non-uniform sampled points in the indirect dimension were recorded (approx. 3 x 1h acquisition time). Inter-scan delay was 0.1 s and 3 x 1024 scans were recorded. The three sets were combined into a single set and processed using maximum entropy reconstruction in the indirect detected dimension [5 3]. To identify signals that arise from protein outside the cells, we carefully transferred the cell suspension from the NMR tube into an eppendorf tube (10 µl was removed for cell count and viability check) and centrifuged at 200 g for 5 min. The resulting supernatant was collected and a SOFAST-HMQC was recorded with 3 x 3072 scans. As a final test for assuring that the signal was from inside the HeLa cells, the pellet from the supernatant preparation was re-suspended and gently sonicated in water bath for 5 min, and after the cell rupture the sample was centrifuged 30 min at 20 000 g. The soluble protein from the cytosol was now in the lysate supernatant and subjected to SOFAST-HMQC analysis as described above (3 x 1024 scans). Cell viability was checked prior and after the NMR analysis by Trypan blue staining [6] and by manually counting the cells. Induced chemical-shift changes were measured as the weighted average shift, defined as $\Delta\delta_{av} = \sqrt{(\Delta\delta_H^2 + \frac{\Delta\delta_N^2}{5})}$.

Fluorescence Microscopy. For fluorescence labelling, CPP-conjugated protein was treated with Alexa-Fluor-488 C5 maleimide (Invitrogen). Non-ligated fluorescent reagent was removed with a PD-10 column (GE Healthcare). HeLa cells were plated into 35 mm glass-bottomed dishes and cultured for 48 h. The cells were then treated first with 50 μM pyrenebutyrate for 5 min, and subsequently with 75 μM Alexa labelled protein in the presence of 50 μM pyrenebutyrate for 10 min. The localisation of the Alexa-labelled protein in the HeLa cells was analysed without fixing, using a confocal laser-scanning microscope (Olympus FV300) equipped with a ×60 objective. The fluorescence signals were detected with a 510–530 nm emission filter using argon-laser excitation at 488 nm.

Folding kinetics. The folding kinetics was measured at 37 °C, pH 6.3, in 10 mM MES-buffer. Protein concentration in the reaction chamber was 4 μM and mixing was by a PiStar-180 stopped-flow apparatus (Applied Photophysics, UK), or manually with detection in a Varian Cary Eclipse spectrometer (Santa Clara, CA, USA), with excitation at 280 nm and emission collected above 305 nm or at 360 nm. Data analysis was with Kaleidagraph (Synergy Software, PA, USA). The observed relaxation rate $\log k_{obs}$ was fitted by standard procedures [1] to

$$\log k_{obs} = \log(k_f + k_u) \qquad \text{(Eq. S1)}$$

where,

$$\log k_f = \log k_f^{H_2O} + m_f[\text{GdmCl}]$$

$$\log k_u = \log k_u^{H_2O} + m_u[\text{GdmCl}]$$

Protein stability, $\Delta G_{U/F} = -RT\ln K_{U/F}$ was calculated as $\Delta G_{U/F} = -2.3RT(\log k_f^{H_2O} - \log k_u^{H_2O})$.

References

(1) Lindberg, M. J.; Normark, J.; Holmgren, A.; Oliveberg, M. *Proc Natl Acad Sci USA* 2004, 101, 15893.
(2) Danielsson, J.; Kurnik, M.; Lang, L.; Oliveberg, M. *J Biol Chem* 2011, *286*, 33070.
(3) Inomata, K.; Ohno, A.; Tochio, H.; Isogai, S.; Tenno, T.; Nakase, I.; Takeuchi, T.; Futaki, S.; Ito, Y.; Hiroaki, H.; Shirakawa, M. *Nature* 2009, *458*, 106.
(4) Schanda, P.; Brutscher, B. *J Am Chem Soc* 2005, *127*, 8014.
(5) Laue, E. D.; Mayger, M. R.; Skilling, J.; Staunton, J. *J Magn Reson* 1986, *68*, 14.
(6) O'Brien, R.; Gottlieb-Rosenkrantz, P. *J Histochem Cytochem* 1970, *18*, 581.